

# A Superposition Model of Droplet and Aerosol Risk in the Transmission of SARS-CoV-2

John E. McCarthy, PhD <sup>1</sup>  
Washington University in St. Louis

Barry D. Dewitt, PhD <sup>2</sup>  
Department of Engineering & Public Policy  
Carnegie Mellon University

Bob A. Dumas, PhD  
Omnium LLC

James S. Bennett, PhD  
Division of Field Studies and Engineering  
National Institute for Occupational Safety and Health, CDC

KEYWORDS: covid-19, bioaerosols, droplets, airborne transmission, respiratory disease

Word count: 2524

May/24/2023

<sup>1</sup>Partially supported by National Science Foundation Grant DMS 2054199

<sup>2</sup>Supported by the Riksbankens Jubileumsfond (Swedish Foundation for the Social Sciences and Humanities) program on Science and Proven Experience

## Abstract

Considering three viral transmission routes – fomites, droplets, and aerosols – two routes have been the focus of debate about the relative role of droplets and aerosols in SARS-CoV-2 infection. We seek to quantify infection risk in an enclosed space via short-range and long-range airborne transmission to inform public health decision making. Data from five published studies were analyzed to predict relative exposure at distances of 1m and farther, mediated by droplet size divided into two bins:  $\geq 8\mu\text{m}$  (medium and large droplets that we call “droplets”) and  $< 8\mu\text{m}$  (small droplets that we call “aerosols”). The results at 1m from an infectious individual were treated as a boundary condition to model infection risk at shorter and longer distance. At all distances, infection risk was treated as the sum of exposure to aerosols and droplets. It was assumed that number of virions is proportional to particle volume. The largest infection risk occurred close to the infectious individual, and out to approximately 1m, droplets and aerosols both contributed. Farther away, the largest risk was due to aerosols. For one model, droplet exposure disappeared at 1.8m. Policy concerning physical distancing for meaningful infection reduction relies on exposure as a function of distance, yet within this construct particle size determines respiratory deposition. This two-fold distance effect can be used to evaluate measures such as plexiglass barriers, masking, and ventilation.

# 1 Introduction

There are believed to be three transmission routes for severe acute respiratory syndrome-coronavirus 2 (SARS-CoV-2): airborne transmission by droplets, airborne transmission by aerosols, and touching eyes, nose, or mouth with a hand that has touched an infected surface (fomite) or person [1]. The airborne routes have been the subject of debate and are clearly important[2], including the distinction between “droplets” and “aerosols” and their relative risk of causing infection [3, 4]. Fennelly [5] emphasizes the pathogen richness of droplets smaller than  $5\text{ }\mu\text{m}$  in cough and exhalation plumes of persons with various respiratory infections, while acknowledging that SARS-CoV-2 is probably transmitted by “small and large particle aerosols.” Prather et al. [6] argue in a letter for a revision from the historical  $5\text{ }\mu\text{m}$  divide between aerosols and droplets to a  $100\text{ }\mu\text{m}$  threshold that better indicates where particle momentum dominates. In W. Chen (2020) [9]  $100\text{ }\mu\text{m}$  is treated as the size where inhalation no longer dominates the short-range exposure. Dividing particles by size into either aerosols or droplets is confounded by the existence of three natural categories—sizes where particles closely follow the airflow; sizes where particles are influenced by the airflow, gravity, and their own momentum; and larger sizes where the effect of airflow is small. Using “aerosol” and “droplets” to denote behavior then corresponds to three behavior regimes: aerosol, aerosol and droplet, and droplet. In the current research, we divide particles into only two size ranges, aerosol ( $< 8\mu\text{m}$ ) and droplets ( $\geq 8\mu\text{m}$ ), with full recognition that defining droplets in this way includes inhalation exposure in much of this size range.

Many previous studies have modeled the complex dynamics of droplets launched from expulsive respiratory events, including host physiology and health state, as it affects droplet size, viscosity, number, and projection [7]. Long before the COVID-19 pandemic, the effects of cough-covering behavior were revealed in smoke visualizations and computational fluid dynamics (CFD), with [8] finding that covering with a tissue, a fist, or the elbow slowed horizontal momentum sufficiently for the droplets to move upward with the body’s thermal plume. A review by [9] of flow visualization techniques demonstrated interactions among the human respiratory and thermal plumes and space airflows in hospital settings. Notably, a Schlieren image showed that a surgical mask stopped the turbulent cough jet from penetrating forward into room air but diverted it upward into the thermal plume. Ai and Melikov [10] reviewed approximately 200 studies and concluded that

boundary conditions, simplifying assumptions, and insufficient time resolution have led to inconsistencies, which require further work in understanding indoor airflow patterns. Added to the variability due to initial conditions and indoor airflows are the many effects of the size of evaporating droplets on trajectory, intake, and viral load [11]. Although most droplets in their model were  $8-16\mu\text{m}$ , they concluded  $32-40\mu\text{m}$  could lead to more infections due to higher viral content. Humidity and temperature affecting droplet size and virus viability was considered in [12], [13], [14], [15], and [16].

A spatially detailed CFD analysis that includes many factors in a simulation of a conversation across a dining table, notably masks and N95 respirators, is reported by [17]. Particle image velocimetry (PIV) validated their simulation. The near field, defined here as within 1m of a respiratory source, has received intense research interest, with measurements often occurring only at 1m. Coldrick et al. [18] extended the range to compare findings at 1m and 2m. CFD models tracked droplets in the warm, humid plume, and experiments assayed bacteria in respiratory and oral droplets generated by human subjects coughing, speaking, and singing. Each approach showed greater deposition of bacteria within 1m and, for droplets smaller than  $10\mu\text{m}$ , no clear difference in airborne concentrations at 1m and 2m. The zone of 0.2 to 2m from the subject was analyzed in a CFD study by [19] that connected two strong themes in COVID-19 research: the importance of the inhalation route of exposure and greater infection risk at close distances.

Distance between a potential infector and a susceptible is clearly important, but distance is a sort of summary variable which contains (and possibly obscures) the time-dynamic biological, chemical, and physical processes occurring as an infectious plume moves outward. Measurement at a specific distance is a snapshot in time when these processes have progressed to an extent toward their resolution. Deconstructing the overall “distance effect” into particle size and exposure route, though difficult, can help to clarify the many terms that have been used throughout the pandemic, such as “close contact” and “aerosol.” In the current study that analyzes published data and models, we combine results at various distances to arrive at some examples of infection risk distance functions. The obvious uncertainty in each piece of such a model constrains the present work to simply be an illustration of placing specific results in a quantitative gestalt.

Although it is now clearer to the broader research community and the public that the threshold between “droplet” and “aerosol” is dynamic [3], depending on both the pathogen and environmental conditions, the relative

importance of droplets and aerosols to infection risks, and the consequences for mitigation policies, is not a settled matter. A report from the UK’s Scientific Advisory Group for Emergencies estimated the risk of SARS-CoV-2 infection for a non-infected person standing at 1m from an infectious person to be at most an order of magnitude larger than the risk of infection at double that distance [20]. We endeavor to improve on estimates of that kind, by comparing the relative viral loads received through standing close to an infectious person with the amount received more generally indoors, such as in classrooms, airplanes, and stadiums. We leverage results from previous empirical research to better model infection risk, potentially as input to risk-cost-benefit analyses of common activities for public and private decision-making [21].

Given that most existing buildings were constructed during decades when the idea of using ventilation to prevent infectious disease was out of favor [22], many built environments can be loci of SARS-COV-2 spread. Here, we attempt to estimate the risks of aerial transmission, operationalized as the quantity of virus in particles exhaled by an infected person and inhaled by a currently uninfected person. We first describe our terminology and the conceptual model. We then incorporate data from the literature to estimate viral loads due to aerial transmission and include estimates derived from bacteriophage droplet tracer studies, for possible exposure during a commercial flight. Finally, we discuss implications for policymaking.

## 2 Methods

### 2.1 Droplets and Virions

Our conceptual model is the following: when an infected person exhales (or vocalizes, coughs or sneezes) they spray a plume of droplets and aerosols that contain the virus into the air. The droplets may collide with a person (including landing on the nose or in the mouth or eyes), be inhaled, land on a surface, or fall to the ground. The aerosols can waft through the air for minutes or hours (depending on the air change rate), travel a long distance, and potentially reach a distant person, where inhalation is the most likely exposure route. We estimate the number of virions dispersed via the respiratory tract of an infected person to be proportional to the initial droplet size as volume. Then, we compare those quantities at different distances to get

a better estimate of the exposure by making a chain of inferences explained at length below.

## 2.2 Data

The terms “droplet” and “aerosol” are often used in the literature with respect to whether they pose *short-range* or *long-range* airborne transmission risk. It is desirable to not require a constant size threshold to separate the particles defined by the two terms, which is a common, but much-criticized, practice [3]. In this study, we do apply a size threshold to align with cited literature that separates droplets into small and medium/large bins.

In Subsection 2.4 we use theoretical results of Chen et al. [23] to estimate the short-range risk from emitted droplets and aerosol. In Subsection 2.5 we use experimental results of Shah et al. [24] to estimate the long-range risk from aerosols for a given rate of aerosol emission. We then use experimental results of Duguid [25] and Chao et al. [26] to estimate what fraction of exhaled particles contributes to risk as aerosols) and what fraction contributes as droplets. Subsection 3.1 compares the risk at distances 1m versus 2m.

## 2.3 Alice and Bob: a Scenario

To provide definitions, list assumptions, and outline the analytical procedure (Figure 1), we use the following scenario: An infectious individual, whom we shall call Alice, poses an airborne infection risk to a non-infected individual, whom we shall call Bob. We proceed as follows:

1. Bob is in an enclosed environment with Alice for an extended period of time (an hour or more). Alice is exhaling saliva and lung fluid droplets of different sizes, all with the same expected concentration of virions per unit volume, initially, at launch. We classify Alice’s droplets into two bins by size.
2. For the purpose of this model, droplets with diameter  $\geq 8\mu\text{m}$  we call *droplets*. These are pulled down by gravity, but slowly for smaller sizes in this range. Using [27] and [28], Maynard [29] reports that a  $58.5\mu\text{m}$  particle falls  $1\text{m}$  in  $10\text{s}$ , in still air. Droplets pose risk to Bob if they land in his mouth, nose or eyes as projectiles. We call this transmission route *Route 1*. They may also be inhaled, and we call this transmission route *Route 2*.

3. Droplets with diameter  $< 8\mu\text{m}$  we call *aerosols*. These drift in the air, where a  $7.4\mu\text{m}$  particle will drop  $1\text{m}$  in 10 min. [Maynard 2020]. The risk they pose to Bob is mainly if he inhales them (Route 2).
4. In Table 1, we give measurements from [26] and [25] of the ratio of volumes for total exhalation in droplets to total exhalation in aerosol. We call this ratio  $\rho$ . The fraction of the total emission of all particles that is aerosol is then  $\frac{1}{\rho+1}$ .
5. From [23], we get that every  $1\mu\text{L}$  of exhaled droplets produces  $17 \times 10^{-6} \mu\text{L}$  of exposure via Route 1 and Route 2 if Bob is facing Alice at a distance of 1m. At this distance the short-range airborne subroute of Chen et al. (our Routes 1 and 2) dominates their large droplet subroute.
6. To extrapolate what the short-range airborne exposure would be at different distances, we use two models: a rapid decay model from [23] and an inverse distance square decrease.
7. For the Route 2 exposure, we use the experimental data of [24]. That study measures what fraction of a given aerosol emission is inhaled at a distance of 2m. We multiply this fraction by  $\frac{1}{\rho+1}$  to estimate the total inhalation of aerosols by Bob via Route 2 at a distance of 2m for every  $1 \mu\text{L}$  of droplets exhaled by Alice.
8. To extrapolate the aerosol inhalation (Route 2) at different distances, we use the bacteriophage measurements in Boeing 737 and 767 aircraft cabin mock-ups of [30].
9. The total exposure of Bob is the sum of the Route 1 and Route 2 exposures. We assume that Bob's risk of infection is proportional to the total exposure.

	Chao Speak	Chao Cough	Duguid Speak	Duguid Cough	Duguid Sneeze
Vol. ( $\mu\text{L}$ ) in Aerosol	3E-06	6E-06	6E-06	1E-04	4E-02
Vol. ( $\mu\text{L}$ ) in Droplets	8E-04	1E-03	5E-03	9E-02	9
Ratio (Droplets/Aerosol)	270	160	760	786	200

Table 1: Volume of various droplet sizes from Chao (2009) [26] (C) and Duguid (1946) [25] (D).

Using the setup described above, we estimate the risks posed by Route 1 and Route 2 exposure in the setting of commercial passenger aircraft.

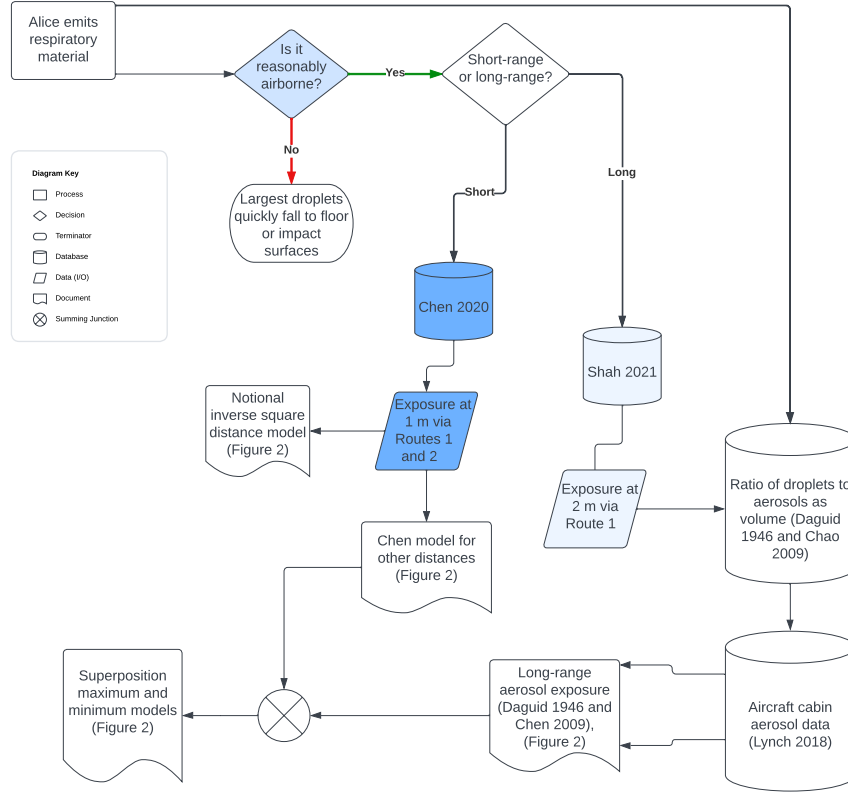


Figure 1: Flowchart illustrating how five published studies (Chen 2020 [23], Duguid 1946 [25], Chao 2009 [26], Shah 2021 [24], Lynch 2018 [30]) are used to form the current model involving distance, particle size (droplets, aerosol) and exposure route (Routes 1 & 2).

## 2.4 Droplet exposure: Routes 1 and 2

In [23], Chen et al. analyze short-range transmission based on a data-driven mathematical model. They assert two main routes of short-range non-fomite transmission: particles that are projected directly into the mouth, nose and



eyes of a nearby facing person at the same height (they ignore droplets that hit any other part of the face or body) and particles that follow the air stream and are inhaled. Large droplets are intrinsically short-range, because gravity pulls them down to the floor in a short period of time (However, if coughed out, they can travel a long distance horizontally.). They conclude that mid-size droplets (defined as having initial diameters of  $75 - 400\mu\text{m}$ ) travel the shortest distance, because they can fall to the ground somewhat rapidly—within 1m (talking) and 2m (coughing), but are too large for airflow carriage over distance and too small for long range ballistic projection. Smaller droplets follow the airflow and travel farther; larger ones have more inertia, so will also travel farther, but will settle to the ground unless they impact another surface. Moreover, they conclude that at distances over 0.3m (talking) and over 0.8m (coughing) the majority of exposure comes from inhaled droplets rather than deposited droplets.

For their base data, [23] use a paper by Duguid [25] that measured the number and size of droplets exhaled by a person coughing, and by counting loudly from 1 to 100. The latter produced a total measured volume of  $0.36\mu\text{L}$  (of which  $2 \times 10^{-3} \mu\text{L}$  came from droplets with a diameter less than  $75\mu\text{m}$ ). The conclusion of [23] that we will use with respect to short-range airborne transmission is that face-to-face, at a range of 1m, a person inhales  $6.2 \times 10^{-6} \mu\text{L}$  of the original  $0.36 \mu\text{L}$  of the talking emission, almost all of it from droplets smaller than  $75 \mu\text{m}$ . Dividing by 0.36 we get that every 1  $\mu\text{L}$  of exhaled droplets produces 17pL of inhaled droplets, via Route 1, from a facing subject at 1m (we change from  $\mu\text{L}$  to pL to make the numbers easier to read and compare).

We shall then multiply the number 17pL by a function depending on distance from the source to get the exposure at different distances. We shall refer to this technique of estimating the exposure at a specific distance and then multiplying by a function that decreases with distance as anchoring. The short-range distance functions decay more rapidly than the long-range ones.

## 2.5 Route 2: Aerosol exposure

In [24], Shah et al. set up a mannikin with a mechanical ventilator that exhaled atomized olive oil droplets, with a mean diameter of  $1 \mu\text{m}$ . The concentration  $c$  of oil in the air was measured for ten hours at a distance of 2 m. Olive oil was chosen because its use with the experimental setup produced

particles of similar sizes to those produced during human exhalation. They fit their results to the following single-box mass balance model:

$$\frac{dc}{dt} = R - \lambda c, \quad (1)$$

where  $c$  is the time-dependent concentration in *particles/m<sup>3</sup>*,  $R$  is the particle injection rate  $R$  in *particles/m<sup>3</sup>s*, and  $\lambda$  is the particle decay rate in  $s^{-1}$ .

Equation (1) simplifies the time-dependent diffusion equation (including sources,  $R$ , and sinks,  $\lambda c$ ), by assuming instantaneous uniform distribution of the aerosols. Operationally, this simplification was made by removing the diffusion term,  $\nabla \cdot K \nabla c$ , where  $K$  is the diffusion coefficient in  $m^2/s$ . Its solution, assuming the initial concentration is zero, is given by

$$c^*(t) = \frac{R^*}{\lambda^*} (1 - e^{-\lambda^* t}). \quad (2)$$

Shah's asterisk notation in Equation (2) is to acknowledge that the injection rate and decay rate in this solution are accounting for some diffusion effects, since there is no explicit diffusion term. The asterisked concentration represents the specific measurement location 2 m from the source, so that Equation 1 need only hold there, rather than throughout the whole space. While the particle source is active, the quantity  $c^*(t)$  from Equation (2) will tend asymptotically to  $c_{\text{sat}}^* = \frac{R^*}{\lambda^*}$ .

Shah et al. [24] measured the concentration of particles at a 2-meter distance from the mannikin, with and without a mask on the source mannikin and at different ventilation rates, indicated as air changes per hour (ACH). Table 2 summarizes some of their results for several masking and ACH combinations.

Mask	ACH	$R^*$ (% $h^{-1}$ )	$\lambda^*$ ( $h^{-1}$ )	$c_{\text{sat}}^* = R^*/\lambda^*$
None	0	$0.53 \pm 0.11$	$0.46 \pm 0.11$	$1.13 \pm 0.057$
Surgical	0	$0.41 \pm 0.36$	$0.41 \pm 0.39$	$0.99 \pm 0.11$
None	1.7	0.48	1.36	0.35
None	3.2	0.41	2.27	0.18

Table 2: Adapted from Shah (2021) [24]. First column indicates whether the exhaling mannikin is wearing a mask. Second column is the number of air changes per hour. Third column is the percentage of exhaled particles that arrive at the detector every hour. Fourth column is the particle loss rate parameter. Fifth column is the steady state or saturation concentration as a percentage of the emission rate.

Thus, for example, at a distance of 2m, they found that the concentration was 1.13% ( $\pm 0.057$  %) of the breath particle injection rate (final column, second row of Table 2). Note that even though the surgical mask material was measured to be 47% effective at blocking particles flowing through it, an amount visible through laser-sheet illumination escaped upward around the bridge of the nose, thus diminishing its effectiveness when worn.

Using the values of  $R^*$  and  $\lambda^*$  from Table 2 and equation 2, we get the estimate at 2m of

$$c^*(t) = 0.0113R(1 - e^{-0.46t}). \quad (3)$$

Equation 3 has little directional dependence: Shah et al. did measure at a distance of 2m and at angles of  $0^\circ$ ,  $90^\circ$  and  $180^\circ$  from the source, and found the variation to be less than 10%.

## 3 Results

### 3.1 Comparing Route 1 and Route 2 exposures

Table 3 shows the aerosol exposure at 2m for a given emission rate. From [23], we get that every 1  $\mu L$  of exhaled droplets produces 17pL of inhaled droplets from a facing subject at 1m. We estimate the long-range risk by first using the values from Table 1 to estimate the fraction of that 1  $\mu L$  that is aerosolized, and then use the data from Table 2 to estimate how much of that is inhaled at steady state conditions at a distance of 2m. We assume an exhaled particle is aerosolized when it has a diameter  $\geq 8 \mu m$ ,

although environmental conditions change the diameter at which particles remain airborne [3].

These assumptions yield the following table. The columns use the measurements from Chao (2009) [26] and Duguid (1946) [25]. The rows are the four conditions in Table 2.

Mask	ACH	Chao Speak	Chao Cough	Duguid Speak	Duguid Cough	Duguid Sneeze
No	0	41	68	14	14	55
Surgical	0	37	61	13	13	49
No	1.7	13	22	4.6	4.5	17
No	3.2	6.7	11	2.4	2.3	9

Table 3: Steady-state aerosol intake in  $pL$  for every  $1 \mu L$  emitted, at a 2m distance from the source (from Chao (2009) [26], Duguid (1946) [25], and Shah (2021) [24]).

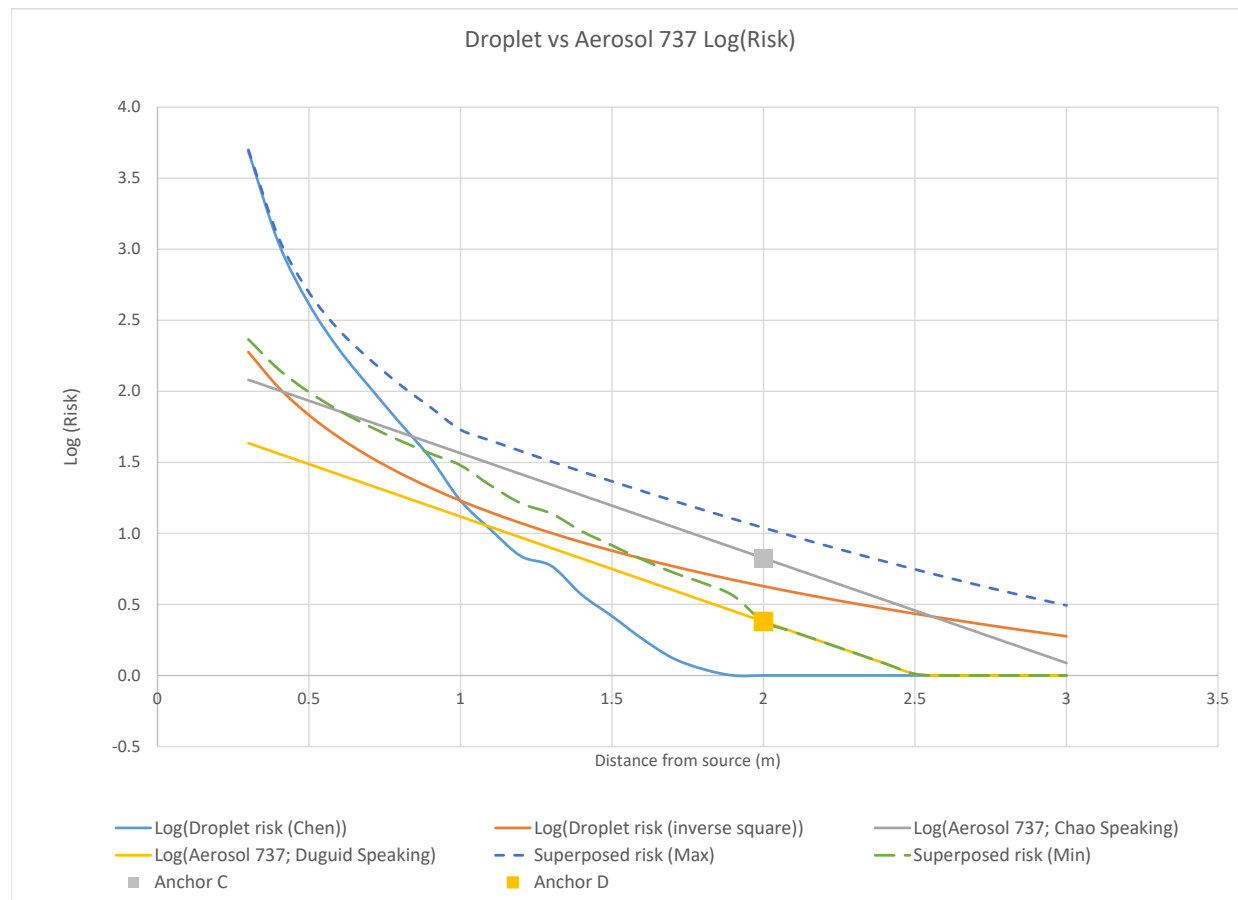
The first entry, for example, is taken by dividing  $1\mu L$  by 271, which Table 1 tells us is the fraction of the original emission that is aerosolized using the measurements from [26] and the assumption that only the small droplets become aerosolized, and then multiplying this number by 1.13% which comes from the last column in Table 2.

### 3.2 Decay with distance

As far as we are aware, no one is certain how the risk from either droplets or aerosols decays with distance from the source. For droplets, the theoretical model of [23] has a very rapid decay with distance. To compare it with a more conservative estimate, we also model the decay as inverse square with distance. We shall anchor the latter with the same exposure at 1m from the Chen et al. model.

For aerosols, the Lynch study [30] of aerosol decay with distance in aircraft cabins reported that their best fit for a single-aisle Boeing 737 was  $e^{-1.7x}$ , where  $x$  is the distance from the source in meters, and for a twin-aisle Boeing 767 it was  $e^{-.47x}$ . Anchoring with the measurement from Table 3 with the largest measured ventilation, 3.2 ACH, the resulting aircraft cabin exponential decay curves plotted on the log scale are the straight lines in Figure 2. The air change rate of the cabins is approximately 32 ACH, ten times

higher than Shah's highest rate, meaning that the rate of aerosol removal was about three times faster. However, the magnitude of these long-range curves (where they are on the vertical axis) is set by the Shah data. In the absence of mechanical ventilation, the decrease of aerosol risk with distance is likely to depend on thermal plumes of occupants and natural infiltration.



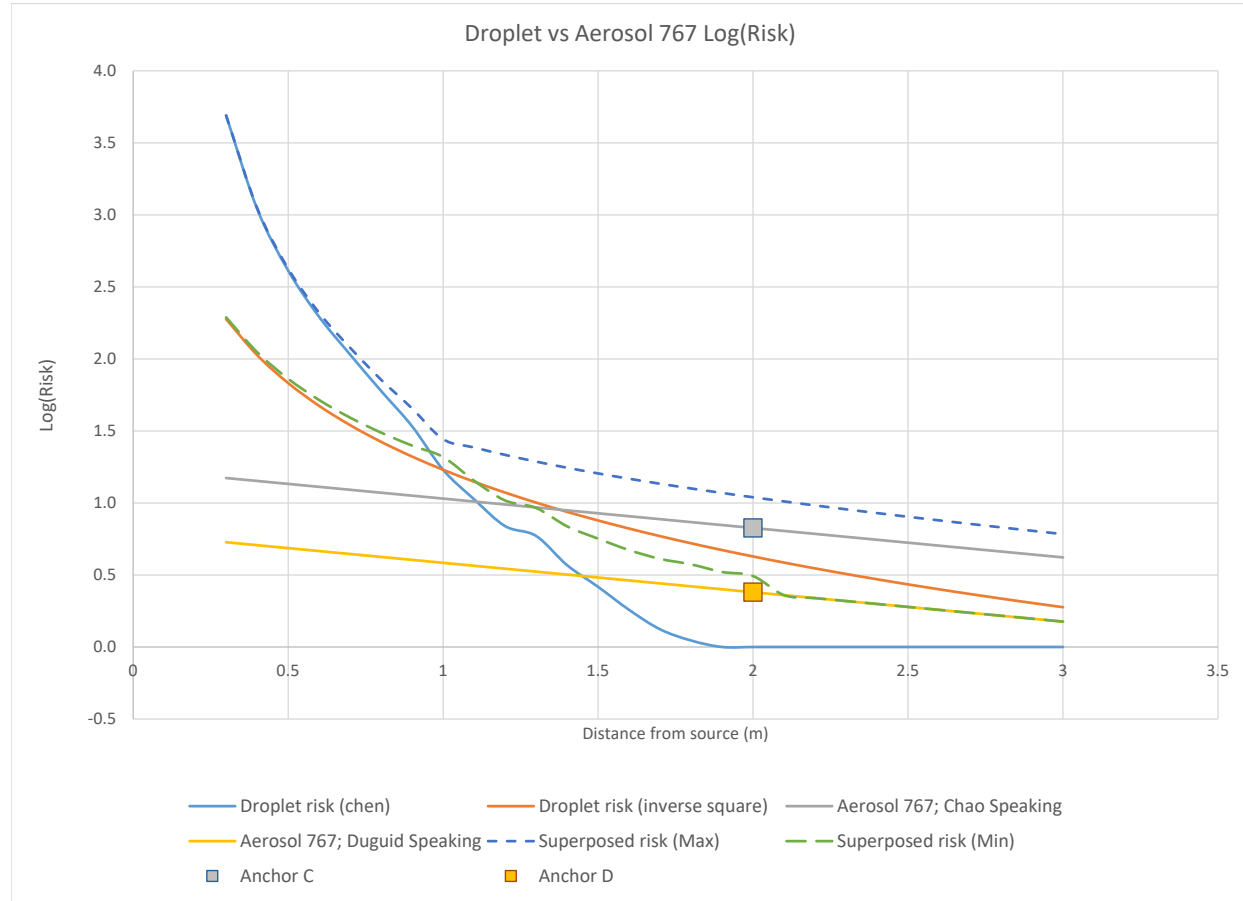


Figure 2: Decrease of risk, as virion exposure, with distance from an infectious person. The key finding is that for short distances both Routes 1 and 2 are important sources of exposure (estimated in two different ways, shown by blue and orange curves), because the decay is steeper than for the long-range models. For these longer distances the primary source of exposure is aerosols and Route 2 (estimated in two different ways, shown by gray and yellow curves). The decrease measured in 737 (first Figure ) and 767 (second Figure) mock-up tracer experiments is normalized or “anchored” to intersect the speaking data at 2m from Chao (gray) and Duguid (yellow). The anchor values from Table 3 are plotted on the log base 10 scale. The superposed risk is the sum of the droplet and aerosol exposure risk. We plot the sum of the maximum and the minimum of the two estimates and note that these are larger than the trend predicted by the long-range data.

## 4 Discussion

Figure 2 shows that selection of effective interventions to reduce exposure must consider how the short- and long-range routes differ. Even these rough estimates based on these models show the relative magnitudes of droplets and aerosol exposures as a function of distance. Starting closest to the source, the very steep descent of Chen’s model (light blue) indicates the presence of droplets, including large ones that fall to the ground within 1 m, unless their launch velocity carries them far as projectiles. This curve slopes downward faster than an inverse square function (orange). More gradual still are the exponential drops of the aircraft cabin curves (straight lines in the log plot). Short-range exposures include direct contact (Route 1) and inhalation (Route 2). Long-range exposures shown by the cabin data represent Route 2. The fact that these distance reduction curves differ greatly suggests Route 2 cannot account by itself for the short-range risk. Therefore, Route 1 must be important. Interventions that mitigate Route 1, such as plexiglass barriers between a customer and a store cashier would then have efficacy; in contrast, Route 2 dominating farther away shows how ventilation, filtration, and air disinfection would be paramount. Of course, interventions such as respirators or masks (worn by both infectious and susceptible) can reduce the risk from both routes.

The superposed exposure curves (dark blue and green) further indicate the importance of Route 1, as these lines are closer to the short-range than they are to the long-range lines. They actually converge to the short-range lines as source distance decreases. The situation is that adding the exposure from Route 2 to the combined exposures from both Routes 1 and 2 makes little difference when within 1 m of the source. One interpretation of this outcome is that direct contact by droplets dominates the total exposure in this short range.

By combining the results from previous empirical and modeling research [26, 23, 25, 30, 24], this study has produced a simple model that aggregates the short-range (i.e., droplet and aerosol) and long-range (i.e., aerosol) airborne risks to produce estimates of virion intake. In Lynch (2018) [12], the aircraft cabin results were generated by visible droplet spray of bacteriophage solution that evaporated to droplet nuclei in the mock-up cabin environment before measurement at distances of 0.5 to 8m. While that generation method produced droplets and aerosol at the source, the measurement distances probably favored aerosol over droplets, certainly over large droplets.

Aircraft cabins and other environments would be better characterized by more measurements close to infection sources, so that this critical zone could be understood in more detail than what is provided by whole-space decay models. The present study is limited by synthesizing results from multiple studies using different methods, and could be improved by data that were all collected using the same experimental procedures.

The estimates of superposed risk from Figure 2 should be compared with Figure 1b in [31], which provides a power law fit to distance for the spatial distribution of droplet mass in an aircraft cabin reported in Zee et al. [32]. Their work modeled a cough source, including evaporation in low humidity cabin air, using computational fluid dynamics.

Our assumption that infection risk is proportional to droplet volume is a limitation. As droplets evaporate and shrink toward their nucleus of possibly infectious material, the number and viability of virions may or may not change. The long-range data from droplet spray in Lynch (2018) [30] consisted mainly of evaporated droplet nuclei, based on the average residence time being longer than the evaporation time. Pease et al. [12] investigated some mechanisms for enveloped viruses such as SARS-CoV-2 to maintain or lose viability. A related weakness is that we relate infection risk directly to exposure taken in, without regard to interactions with tissue, infection thresholds, and individual susceptibility.

All of the estimates presented here highlight the importance of mask use by all persons, which lowers the risks to those close to an infected person [33] and at greater distances. Estimates of virion intake depended on the model used (Figure 2); and, given uncertainties in viral-shedding and in how infection risk scales with exposure duration [34], the continued use of requirements (i.e., masks, vaccination, testing) for persons who choose to participate in optional activities near others is justifiable. When the infectivity of nearby occupants is unknown and unchangeable, such as on commercial airplanes or at sporting events with full seating, perhaps no personally-chosen mitigation is available beyond wearing a high-quality mask. Fundamentally, Figure 2 show that physical distancing reduces exposure from both short- and long-range routes and should be considered as an administrative control layer within the prevention strategy.



## 5 Conclusion

The importance of droplets and aerosol in SARS-CoV-2 infection has been the focus of debate, and we have provided some quantification of the relative roles of these size ranges. Using five published studies, we have developed a model that suggests the largest infection risk (as exposure to droplet volume) came from droplets (particles of  $8\mu\text{m}$  and larger), when close to the infectious individual out to approximately 1m. Farther away, the largest risk was due to aerosols (particles smaller than  $8\mu\text{m}$ ). Because the risk exposure by particle size has been estimated in different ways, and moreover depends on varying environmental and spatial characteristics, we cannot say exactly at what distance aerosol and associated mechanisms become the primary source of exposure, but it seems to be approximately 1m.

That droplets are important close to a source comes as no surprise, when droplet inhalation is recognized as an exposure route that contributes along with direct contact to short-range risk, but verification of this intuition is a step toward focusing public health measures. These trends emerged while summing the contributions of both size ranges to estimate the total exposure. Policy concerning physical distancing for meaningful infection reduction relies on exposure as a function of distance, yet within this construct particle size determines respiratory deposition. This two-fold distance effect can be used to evaluate additional measures such as plexiglass barriers, masking, and ventilation. Duguid’s observation in 1946 about collecting respiratory droplets on glass slides is relevant today, for the uses and limitations of barriers: “Few droplets were found of less than  $10\mu\text{m}$  in diameter and none of less than  $5\mu\text{m}$ . It is presumed that droplets smaller than this possessed such a small mass, or evaporated rapidly to such a small mass, that they were carried past the slide in the deflected air stream.”

## References

- [1] CDC. How COVID-19 Spreads. <https://www.cdc.gov/coronavirus/2019-ncov/prevent-getting-sick/how-covid-spreads.html>, 2021.
- [2] Trisha Greenhalgh, Jose L. Jimenez, Kimberly A. Prather, Zeynep Tufekci, David Fisman, and Robert Schooley. Ten scientific reasons in support of airborne transmission of SARS-CoV-2. *The Lancet*, 397(10285):1603–1605, 2021.

- [3] K Randall, E T Ewing, Linsey C Marr, J L Jimenez, and L Bourouiba. How did we get here: what are droplets and aerosols and how far do they go? A historical perspective on the transmission of respiratory infectious diseases. Interface Focus, 11(6):1–17, dec 2021.
- [4] Prateek Bahl, Con Doolan, Charitha de Silva, Abrar Ahmad Chughtai, Lydia Bourouiba, and C Raina MacIntyre. Airborne or Droplet Precautions for Health Workers Treating Coronavirus Disease 2019? The Journal of Infectious Diseases, pages 1–8, 2020.
- [5] Kevin P Fennelly. Particle sizes of infectious aerosols: implications for infection control. The Lancet Respiratory Medicine, 8(9):914–924, 2020.
- [6] Kimberly A. Prather, Linsey C. Marr, Robert T. Schooley, Melissa A. McDiarmid, Mary E. Wilson, and Donald K. Milton. Airborne transmission of sars-cov-2. Science, 370(6514):303–304, 2020.
- [7] D. Fontes, J. Reyes, K. Ahmed, and M. Kinzel. A study of fluid dynamics and human physiology factors driving droplet dispersion from a human sneeze. Physics of Fluids, 32(11), 11 2020. 111904.
- [8] C. Chen, C.-H. Lin, Z. Jiang, and Q. Chen. Simplified models for exhaled airflow from a cough with the mouth covered. Indoor Air, 24(6):580–591, 2014.
- [9] J.W. Tang, C.J. Noakes, P.V. Nielsen, I. Eames, A. Nicolle, Y. Li, and G.S. Settles. Observing and quantifying airflows in the infection control of aerosol- and airborne-transmitted diseases: an overview of approaches. Journal of Hospital Infection, 77(3):213–222, 2011. Proceedings from the Sporicidal Workshop.
- [10] Z. T. Ai and A. K. Melikov. Airborne spread of expiratory droplet nuclei between the occupants of indoor environments: A review. Indoor Air, 28(4):500–524, 2018.
- [11] H. Li, F.Y. Leong, G. Xu, and et al. Airborne dispersion of droplets during coughing: a physical model of viral transmission. Sci Rep, 11:4617, 2021.
- [12] Leonard F. Pease, Na Wang, Gourihar R. Kulkarni, Julia E. Flaherty, and Carolyn A. Burns. A missing layer in covid-19 studies:

- Transmission of enveloped viruses in mucus-rich droplets. International Communications in Heat and Mass Transfer, 131:105746, 2022.
- [13] E. P. Vejerano and L. C. Marr. Physico-chemical characteristics of evaporating respiratory fluid droplets. 15(139), 2018.
  - [14] Andrea J. French, Alexandra K. Longest, Jin Pan, Peter J. Vikesland, Nisha K. Duggal, Linsey C. Marr, and Seema S. Lakdawala. Environmental stability of enveloped viruses is impacted by initial volume and evaporation kinetics of droplets. 14(2), 2023.
  - [15] E. Mikhailov, S. Vlasenko, R. Niessner, and U. Pöschl. Interaction of aerosol particles composed of protein and salts with water vapor: hygroscopic growth and microstructural rearrangement. Atmospheric Chemistry and Physics, 4(2):323–350, 2004.
  - [16] Wan Yang, Subbiah Elankumaran, and Linsey C. Marr. Relationship between humidity and influenza a viability in droplets and implications for influenza’s seasonality. PLoS One, 2012.
  - [17] David Engler Faleiros, Wouter van den Bos, Lorenzo Botto, and Fulvio Scarano. Tu delft covid-app: A tool to democratize cfd simulations for sars-cov-2 infection risk analysis. Science of The Total Environment, 826:154143, 2022.
  - [18] Simon Coldrick, Adrian Kelsey, Matthew J. Ivings, Timothy G. Foat, Simon T. Parker, Catherine J. Noakes, Allan Bennett, Helen Rickard, and Ginny Moore. Modeling and experimental study of dispersion and deposition of respiratory emissions with implications for disease transmission. Indoor Air, 32(2):e13000, 2022.
  - [19] W. Chen, L. Liu, J. Hang, and et al. Predominance of inhalation route in short-range transmission of respiratory viruses: Investigation based on computational fluid dynamics. Build. Simul., 16:765–780, 2023.
  - [20] Scientific Advisory Group for Emergencies. Transmission of SARS-CoV-2 and Mitigating Measures. Technical Report June, 2020.
  - [21] John E. McCarthy, Barry D. Dewitt, Bob A Dumas, and Myles T. McCarthy. Modeling the relative risk of SARS-CoV-2 infection to inform risk-cost-benefit analyses of activities during the SARS-CoV-2 pandemic. PLOS ONE, 16(1):e0245381, jan 2021.

- [22] Lidia Morawska, Joseph Allen, William Bahnfleth, Philomena M. Bluysen, Atze Boerstra, Giorgio Buonanno, Junji Cao, Stephanie J. Dancer, Andres Floto, Francesco Franchimon, Trisha Greenhalgh, Charles Haworth, Jaap Hogeling, Christina Isaxon, Jose L. Jimenez, Jarek Kurnitski, Yuguo Li, Marcel Loomans, Guy Marks, Linsey C. Marr, Livio Mazzarella, Arsen Krikor Melikov, Shelly Miller, Donald K. Milton, William Nazaroff, Peter V. Nielsen, Catherine Noakes, Jordan Peccia, Kim Prather, Xavier Querol, Chandra Sekhar, Olli Seppänen, Shin Ichi Tanabe, Julian W. Tang, Raymond Tellier, Kwok Wai Tham, Pawel Wargocki, Aneta Wierzbicka, and Maosheng Yao. A paradigm shift to combat indoor respiratory infection. Science, 372(6543):689–691, 2021.
- [23] Wenzhao Chen, Nan Zhang, Jianjian Wei, Hui-Ling Yen, and Yuguo Li. Short-range airborne route dominates exposure of respiratory infection during close contact. Building and Environment, 176:106859, jun 2020.
- [24] Yash Shah, John W. Kurelek, Sean D. Peterson, and Serhiy Yarusevych. Experimental investigation of indoor aerosol dispersion and accumulation in the context of covid-19: Effects of masks and ventilation. Physics of Fluids, 33(7):073315, 2021.
- [25] JP Duguid. The size and the duration of air-carriage of respiratory droplets and droplet-nuclei. Epidemiol. Infect., 44(6):471–479, 1946.
- [26] C.Y.H. Chao, M.P. Wan, L. Morawska, G.R. Johnson, Z.D. Ristovski, M. Hargreaves, K. Mengersen, S. Corbett, Y. Li, X. Xie, and D. Katoshevski. Characterization of expiration air jets and droplet size distributions immediately at the mouth opening. Journal of Aerosol Science, 40(2):122–133, 2009.
- [27] William C. Hinds. Aerosol Technology: Properties, Behavior, and Measurement of Airborne Particles. Wiley, 1982.
- [28] PA Baron. Description of an aerosol calculator. In Biswas P., Chen D.R., and Hering S., editors, Proceedings of the Seventh International Aerosol Conference, September 10-15, 2006, St. Paul, Minnesota, USA. American Association for Aerosol Research, Mount Laurel, NJ, 2006.
- [29] Andrew Maynard. <https://hiddenworld.andrewmaynard.me/2020/07/17/how-long-do-aerosols-stay-airborne/>, 2020.

- [30] J.A. Lynch, J.S. Bennett, B.W. Jones, and M.H. Hosni. Viral particle dispersion and viability in commercial aircraft cabins. 2018 ASHRAE annual conference Proceedings, 2018.
- [31] J.S. Bennett, S. Mahmoud, W. Dietrich, B. Jones, and M. Hosni. Evaluating vacant middle seats and masks as coronavirus exposure reduction strategies in aircraft cabins using particle tracer experiments and computational fluid dynamics simulations. 2022.
- [32] M. Zee, A.C. Davis, A.D. Clark, T. Wu, S.P. Jones, L. L. Waite, J.J. Cummins, and N.A. Olson. Computational fluid dynamics modeling of cough transport in an aircraft cabin. Sci Rep, (11), 2021.
- [33] Gholamhossein Bagheri, Birte Thiede, Bardia Hejazi, Oliver Schlenczek, and Eberhard Bodenschatz. An upper bound on one-to-one exposure to infectious human respiratory particles. Proceedings of the National Academy of Sciences, 118(49):e2110117118, 2021.
- [34] Nicholas R. Jones, Zeshan U. Qureshi, Robert J. Temple, Jessica P.J. Larwood, Trisha Greenhalgh, and Lydia Bourouiba. Two metres or one: what is the evidence for physical distancing in covid-19? BMJ (Clinical research ed.), 370:m3223, 2020.

The findings and conclusions in this report are those of the authors and do not necessarily represent the official position of the National Institute for Occupational Safety and Health, Centers for Disease Control and Prevention.